Virus Research 339 (2024) 199258

Contents lists available at ScienceDirect

Virus Research

journal homepage: www.elsevier.com/locate/virusres

Tetrandrine (TET) inhibits African swine fever virus entry into cells by blocking the PI3K/Akt pathway

Bingxu Qian [a,b], Yongxin Hu [b], Cong Liu [a], Dongxia Zheng [b], Xiuju Han [b], Mingxia Gong [b], Yanli Zou [b], Dexin Zeng [d,e], Kai Liao [a], Yurun Miao [a], Xiaodong Wu [b,**], Jianjun Dai [a], Zhiliang Wang [b,**], Feng Xue [a,c,*]

[a] National Key Laboratory of Meat Quality Control and New Resource Creation, Nanjing Agricultural University, Nanjing, China
[b] China Animal Health and Epidemiology Center, Qingdao, China
[c] Sanya Institute of Nanjing Agricultural University, Sanya, China
[d] Technical Center of Hefei Customs, Hefei, China
[e] Technology Center of Hefei Customs, and Anhui Province Key Laboratory of Analysis and Detection for Food Safety, Hefei, China

ARTICLE INFO

Keywords:
African swine fever virus
Tetrandrine
Macropinocytosis
PI3K/Akt
Broad-spectrum antiviral drug

ABSTRACT

African Swine Fever Virus (ASFV) infection causes an acute and highly contagious disease in swine, resulting in significant economic losses and societal harm worldwide. Currently, there are no effective vaccines or antiviral drugs available for ASFV. Tetrandrine (TET) is extracted from the traditional Chinese herb Stephania tetrandrae, possesses diverse biological functions such as anti-inflammatory, anti-tumor, and antiviral activities. The study comprehensively evaluated the anti-ASFV effect of TET and validated it through biological assays. The dose-dependent inhibition of TET against ASFV was confirmed and a novel mechanism of TET's anti-ASFV activity was elucidated. TET effectively inhibits ASFV during internalization by blocking macropinocytosis through the inhibition of the PI3K/Akt pathway. The specific inhibitor LY294002, targeting the PI3K/Akt pathway, exhibits similar antiviral activity against ASFV as TET. Furthermore, the inhibitory effect of TET against other viruses such as Lumpy Skin Disease Virus (LSDV) and Porcine Epidemic Diarrhea Virus (PEDV) was also identified. Our findings suggest that TET effectively inhibits ASFV and reveal the potential for broad-spectrum antiviral drugs targeting the PI3K/Akt pathway.

1. Introduction

African swine fever (ASF), a contagious haemorrhagic viral disease caused by the African swine fever virus (ASFV), was first reported in Kenya in 1921 (Eustace Montgomery, 1921). ASFV is a linear double-stranded DNA virus with a genome length of 170–193 kb, which encodes 150 to 170 open reading frames (ORFs) (Cackett et al., 2020). The virus has icosahedral symmetry with a diameter of about 200 nm and is composed of five layers: Nucleoid, Core shell, Inner envelope, Capsid and Outer membrane (Xian and Xiao, 2020). ASFV only infects domestic pigs and wild boars, and can cause hemorrhagic fever up to 41 °C within 3–4 days of post infection (Dixon et al., 2019). ASF poses significant health and socioeconomic hazards to international trade in swine products due to its high mortality rate (Gallardo et al., 2015). Since 2016, there has been a global rise in the epidemic of ASF, with over 30 % of countries and regions around the world reporting ASF cases. In August 2018, ASF was introduced into China and spread rapidly (Ge et al., 2018). Currently, there are no effective vaccines or

Abbreviations: TET, tetrandrine; CPZ, chlorpromazine; AMI, amiloride; HRP, horseradish peroxidase; ASF, African swine fever; ASFV, African swine fever virus; LSDV, lumpy skin disease virus; PEDV, porcine epidemic diarrhea virus; BSL-3, biological safety protection third-level laboratory; ORFs, open reading frames; BBI, bisbenzyl isoquinoline alkaloid; DMSO, dissolved in dimethyl sulfoxide; N, nucleocapsid; IFA, indirect immunofluorescence assay; PAMs, porcine alveolar macrophages; FBS, fetal bovine serum; CC_{50}, median cytotoxic concentration; IC_{50}, median inhibitory concentration; qRT-PCR, quantitative reverse transcription PCR; TOA, time of addition; MOI, multiplicity of infection; HAD_{50}, hemoadsorption assay; PI3K/Akt, phosphatidylinositol 3 kinase/protein kinase B; TPCs, two-pore channels.

* Corresponding author at: National Key Laboratory of Meat Quality Control and New Resource Creation, Nanjing Agricultural University, Nanjing, China.
** Corresponding authors.
E-mail addresses: wuxiaodong@cahec.cn (X. Wu), wangzhiliang@cahec.cn (Z. Wang), xuefeng@njau.edu.cn (F. Xue).

https://doi.org/10.1016/j.virusres.2023.199258
Received 17 July 2023; Received in revised form 26 October 2023; Accepted 27 October 2023

antiviral drugs against ASFV. Therefore, the development and screening of antiviral drugs against ASFV are crucial for the prevention and control of epidemics.

Tetrandrine (TET), a bisbenzyl isoquinoline alkaloid (BBI), was originally discovered in a Japanese medicinal plant by Chen and Chen (1935). It is a versatile natural product that can be extracted from various Chinese herbal medicines, including *Cyclica Barbata*, menispermaceous plants, and *Stephania Cepharantha Hayata* (Wang et al., 2021). TET, acting as a calcium channel blocker, has found widespread clinical applications in the treatment of silicosis, autoimmune disorders, inflammatory pulmonary diseases, cardiovascular diseases, and hypertension (Liu et al., 2016). The efficacy of TET was confirmed against *Mycobaterium tuberculosis, Candida albicans, Plasmodium falciparum* and Ebola virus (Bhagya and Chandrashekar, 2016).

Previous studies have reported the anti-ASFV activity of TET, but these studies utilized the ASFV BA71V strain, which belongs to genotype I and is not the currently prevalent dominant strain (Galindo et al., 2021). Here, we tested the antiviral activity of TET against genotype II ASFV in vitro and explored its inhibitory mechanisms.

2. Materials and methods

2.1. Cells, virus and drugs

Porcine alveolar macrophages (PAMs) were obtained from the lungs of 4-week-old specific pathogen-free pigs by PBS irrigation. Bone marrow-derived macrophages (BMDMs) were obtained from the femur and tibia of pigs. MA104, Vero, MDBK and IPEC-J2 cells were preserved in Nanjing Agricultural University. The ASFV strain used was China/2018/AnhuiXCGQ (GenBank accession no. **MK128995.1**), and the virus titer was determined to be $10^{6.29}$ HAD_{50}/mL using the Spearman–Karber method. Tetrandrine (S2403), Chlorpromazine (CPZ, S2456) and Amiloride (AMI, S1811) were purchased from Selleck Chemicals (Houston, USA), it was dissolved in dimethyl sulfoxide (DMSO) at storage concentration and resuspended in DMEM without FBS at indicated concentrations for further use. At the time of experiments, dilutions in cell culture medium were performed with the final concentration of DMSO not exceeding 1 % (v/v). All operations involving ASFV in the present study were carried out in the biological safety protection third-level laboratory (BSL-3) at the National Research Center for Exotic Animal Diseases, China Animal Health and Epidemiology Center (Qingdao, China).

2.2. Antibodies and reagents

The mouse monoclonal antibody ASFV-p72 and ASFV-p30 were deposited in the National Research Center for Exotic Animal Diseases, China Animal Health and Epidemiology Center. The mouse monoclonal antibody of LSDV-117 protein and PEDV nucleocapsid (N) protein were prepared and stored in laboratory of Veterinary Medicine College of Nanjing Agricultural University. Goat Anti-Mouse IgG (H + L) FITC (BS50950), HRP-labeled goat anti-mouse IgG (BS12478) and HRP-labeled goat anti-rabbit IgG (ZJ2020-R) were purchased from Bioworld Technology. Inc (Nanjing, China). Rabbit polyclonal beta actin antibody (20536-1-AP) was purchased from Proteintech Group, Inc (Chicago, USA). CCK8 cytotoxicity kit (C0037) was purchased from APExBIO Technology LLC (Houston, USA). SuperBlock™ Blocking Buffer (37,515), Pierce™ ECL Western Blot Substrate (32,209), Lipofectamine® LTX & PLUS™ Reagent (15,338), Transferrin-Alexa594 (T13343) and Dextran-Alexa647 (D22914) were purchased from ThermoFisher Scientific (Massachusetts, USA). FastPure® Cell/Tissue Total RNA Isolation Kit V2 (RC112), HiScript II 1st Strand cDNA Synthesis Kit (+gDNA wiper) (R212) and AceQ® qPCR SYBR Green Master Mix (High ROX Premixed) (Q141) were all purchased from Vazyme Biotechnology (Nanjing, China). RIPA lysis buffer (P0013B), 1 % protein inhibitor (P1006), bicinchoninic acid Protein Assay Kit (P0009) and DAPI (C1002) were all purchased from Beyotime Biotechnology (Shanghai, China). Polyvinylidene fluoride (PVDF) membranes were purchased from Millipore (Billerica, MA, USA). Akt Antibody (9272S) and Phospho-Akt (Ser473) (D9E) XP® Rabbit mAb (4060) were purchased from Cell Signaling Technology (Danvers, MA, USA). The broad-spectrum PI3K inhibitor LY294002 (HY-10108) was purchased from MedChemExpress (New Jersey, USA).

2.3. Cell cytotoxicity assay

The cytotoxicity of TET to cells was determined using CCK8 assay. The cells were distributed in 96-well plates, and after the cells had fully adhered to the plate walls, TET diluted in medium containing 10 % fetal bovine serum (FBS) was added at different final concentrations. The experiments included a sample group treated with TET treatment, a negative control without TET treatment and a blank control without cells, and all groups contained three replicates. After incubating cells for 48 h, 10 μL of CCK8 was added and incubated for 1 h, the absorbance was measured at 450 nm. Cell viability was calculated as per the following formula: Cell viability = [(OD sample − OD blank)/(OD negative − OD blank)] × 100 %. The drug concentration leading to 50 % concentration of cytotoxicity (CC_{50}) was fitting calculated using GraphPad Prism 8 software (GraphPad, Inc., La Jolla, CA, USA).

2.4. Indirect immunofluorescence assay (IFA)

After pre-treating PAMs cells with TET for 2 h, PAMs were infected with 1 MOI ASFV for 24 h. Following this, the residual culture medium in the wells was removed by washing with PBS, and the cells were subsequently fixed with paraformaldehyde (4 %) at room temperature for 15 min. The cells were thoroughly washed thrice with PBS and permeabilized with 0.25 % Triton X-100 for 10 min. To block nonspecific binding, SuperBlock™ Blocking Buffer was added and incubated at 37 °C for 1 h after three additional washes. The samples were then incubated with the p72 antibody (1:500) at 37 °C for 1 h and washed thrice with PBS. Goat Anti-Mouse IgG (H + L) FITC (1:200) was added and incubated in the dark at 37 °C for 1 h. The fixed cells were stained with 4′,6-diamidino-2-phenylindole (DAPI) for 10 min in the dark and observed using a Leica DMI 4000B fluorescence microscope (Leica, Oskar, Germany).

2.5. 50 % inhibitory concentration (IC_{50})

PAMs and BMDMs were seeded in 96-well cell plates at a density of 2 × 10^4 cells/well, while MA104 cells were seeded at a density of 1 × 10^4 cells/well. After the cells were fully attached to the wall, 2 h of pre-treatment with TET at concentration gradients of 2, 1, 0.5, and 0.25 μM. Following the pre-treatment, cells were infected with ASFV [multiplicity of infection (MOI) = 1] for 24 h. Positive control was set up for ASFV-infected cells, while negative control was neither infected with ASFV nor treated with TET. After fixing the cells with 4 % paraformaldehyde at room temperature for 15 min, primary p30 monoclonal antibody (1:2500) and secondary goat anti-mouse antibody (1:10,000) were used for Cell-ELISA assay. The OD values were measured, and the inhibitory rate of TET against ASFV on PAMs, BMDMs or MA104 cells was determined using the formula: Inhibitory rate = [(OD positive − OD sample)/(OD positive − OD negative)] × 100 %. IC_{50} was fitting calculated using GraphPad Prism 8 software.

2.6. Time of addition (TOA) assays

The ASFV infection was divided into three stages: attachment, internalization and replication. To evaluate the therapy stage of TET on virus infection, 8 groups (Fig. 3(A)) were split according to different treatment methods of TET (Van Loock et al., 2013). These groups comprise the entire life cycle of ASFV to rapidly determine the therapy

stage of TET in viral infection. PAMs (2×10^6 cells/well) were cultured in a 12 well cell culture plate. The attachment phase involves pre-treating PAMs with 2 μM TET before ASFV infection. In the internalization phase, ASFV (MOI = 1) and 2 μM TET are added simultaneously to PAMs. The replication phase entails the addition of 2 μM TET after ASFV has entered the PAMs.

2.7. The impact of co-incubation of TET and ASFV on infection

ASFV and TET at concentrations of 0 μM, 2 μM, and 4 μM were co-incubated at 37 °C for 1 h, followed by the infection of PAMs with the TET-treated ASFV. Concurrently, PAMs were pretreated with TET as a control for ASFV infection. After 24 h of ASFV infection, RNA was extracted for qRT-PCR assay.

2.8. ASFV infection and RNA interference

All siRNAs and siRNA control (si-Ctrl) were designed and synthesized by Tsingk (Nanjing, China) and listed in Table 1 (Chen et al., 2023). In knockdown experiments, PAMs were transfected with siRNA negative controls or siRNAs as indicated at a final concentration of 10 nM using Lipofectamine LTX according to the manufacturer's instructions. 24 h after transfection, cells were infected with ASFV (MOI = 1) for 24 h. The total RNA of PAMs was extracted for qRT-PCR assay.

2.9. Quantitative reverse transcription PCR (qRT-PCR)

Total RNA was extracted from the cells using FastPure® Cell/Tissue Total RNA Isolation Kit V2 and reverse-transcribed into cDNA using HiScript II 1st Strand cDNA Synthesis Kit (+gDNA wiper). The cDNAs were used as templates for qRT-PCR on a CFX96 Optics Module (Bio–Rad, Hercules, CA, USA) using AceQ® qPCR SYBR Green Master Mix (High ROX Premixed). The expression of mRNA was assessed in each sample in triplicate, and Beta-actin was used as an endogenous negative control. The expression of each target gene was calculated using the $2^{-\Delta\Delta CT}$ method. The sequences of the primers and probes used in this study are listed in Table 1.

2.10. Western Blot

The cells were thoroughly washed twice with cold PBS before being lysed with RIPA lysis buffer containing 1 % protein inhibitor. In order to guarantee uniform protein loading, the overall protein concentration of each specimen was measured utilizing the Bicinchoninic Acid Protein Assay Kit. The proteins were then separated by polyacrylamide gel electrophoresis technique and transferred onto PVDF membranes. The PVDF membranes were blocked with SuperBlock™ Blocking Buffer before being incubated with the primary antibody. The HRP-labeled goat anti-mouse IgG or goat anti-rabbit IgG was used as the secondary antibody. The presence of proteins on the PVDF membranes was visualized using the Pierce™ ECL Western Blot Substrate. Finally, a Tanon-5200 Multi Infrared imaging system (Shanghai Tanon Technology) was utilized to analyze the protein staining.

Table 1
The sequence of siRNA and primers used in this study.

Primer	Sequence (5′–3′)
si-CD1d-245	GCAAUGACUCGGACACCAUTT
si-CD1d-421	GCUGGAUGUGAGGUGCUUUTT
si-Ctrl	UUCUCCGAACGUGUCACGUTT
B646L-F	GGTTGGTATTCCTCCCGTGG
B646L-R	GCAGCTCTTACATACCCTTCCA
CD1d-F	CACTCAGCATTTCAAGGAACAGACATC
CD1d-R	TCCTCGTTGAGCACTCTACAGACC
β-actin-F	CACGCCATCCTGCGTCTGGA
β-actin-R	AGCACCGTGTTGGCGTAGAG

2.11. Endocytosis assay

The PAMs were seeded at a density of 2×10^6 cells/well in 12-well plates containing sterilized cell slides. After allowing the cells to attach completely, the culture medium was discarded, and serum-free DMEM was added for a 2 h starvation treatment at 37 °C to prevent serum interference with the internalization of transferrin-Alexa594 or dextran-Alexa647. Subsequently, the medium was subsequently removed, and a 20 μg/mL solution of transferrin-Alexa594 or dextran-Alexa647 was added. The cells were then incubated at 37 °C for 45 min. The culture medium was discarded to terminate the internalization and remove transferrin-Alexa594 or dextran-Alexa647 from the cell membrane surface. Subsequently, a 4 % paraformaldehyde solution was added and the cells were fixed at room temperature for 15 min. The cells were then washed twice with PBS containing 0.02 M Glycine, followed by three washes with PBS. Finally, the cells were stained with DAPI solution for nuclear staining and coverslips were applied.

2.12. Virus attachment assay

To evaluate the impact of viral attachment on the phosphatidylinositol 3 kinase/protein kinase B (PI3K/Akt) pathway, a 12-well cell plate containing MA104 cells (1×10^5 cells/well) was pre-incubated at 4 °C for 1 h. Subsequently, the cells were incubated with ASFV (MOI = 1) at 4 °C, allowing ASFV binding but prevent virus internalization. Multiple time points were set, and protein samples were collected to analyze the effects of ASFV attachment on the PI3K/Akt pathway by Western Blot.

2.13. Hemoadsorption assay (HAD_{50})

PAMs were seeded in a 96-well cell plate and allowed to adhere. Once the cells were fully attached, they were pre-treated with TET for 2 h. Following the pre-treatment, the ASFV virus solution was diluted to different concentrations (10^{-1}, 10^{-2}, 10^{-3}, 10^{-4}, 10^{-5}, 10^{-6}, 10^{-7}, 10^{-8}). Eight replicates per dilution were added to the PAMs and incubated for 1 h. After incubation, the cell supernatant was discarded. ASFV was introduced at a 1 MOI for 1 h, after which the cell supernatant was discarded. Subsequently, 20 μL of 0.5 % porcine red blood cells were added to each well to evaluate the hemoadsorption of ASFV-infected erythrocytes. The HAD_{50} was determined using the Spearman–Karber method to measure the virus titer (Knudsen et al., 1987).

2.14. Statistical analysis

In this study, statistical calculations and data plotting were performed using GraphPad Prism 8.0. Differences between two independent samples were assessed using two-tailed Student's *t*-tests. Differences between multiple samples were analyzed using one-way analysis of variance (ANOVA). Data is presented as the mean ± SD. We considered $P < 0.05$ to be statistically significant. Significance values were set as follows: ns (not significant), $P > 0.05$; ****, $P < 0.0001$; ***, $P < 0.001$; **, $P < 0.01$; *, $P < 0.05$.

3. Results

3.1. Cytotoxicity of TET towards cells

The molecular formula of TET is depicted in Fig. 1(A), and its cytotoxicity toward PAMs, BMDMs and MA104 cells was evaluated using the CCK-8. Notably, after 48 h of incubation, high concentrations of TET exhibited obvious cytotoxicity on both cells, with cell viability below 30 % for PAMs and BMDMs and below 40 % for MA104 cells at a TET concentration of 25 μM. However, when the TET concentration was below 5 μM, the cell viability exceeded 80 % for BMDMs and 90 % for both PAMs and MA104 cells, and there were no apparent differences in cell morphology compared to the untreated control group (Fig. 1(B)).

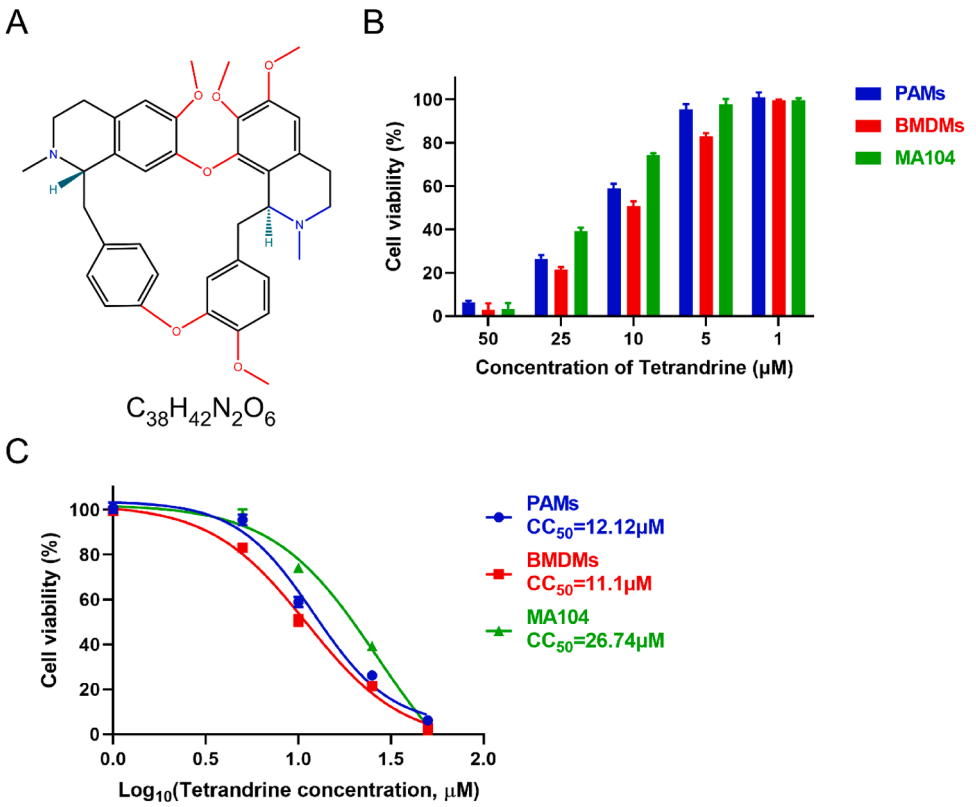

Fig. 1. Cytotoxicity and CC_{50} of TET on PAMs, BMDMs and MA104 cells. (A) Chemical structure of TET. (B) Cytotoxicity of TET toward PAMs, BMDMs and MA104 cells was analyzed by CCK-8 assay. The relative viability of PAMs, BMDMs or MA104 cells cultured without TET was set to 100 %. Each value represents the average of three independent experiments. (C) CC_{50} of TET in PAMs, BMDMs and MA104 cells was calculated, respectively.

The CC_{50} of TET in PAMs is 12.12 μM, in BMDMs is 11.1 μM, and in MA104 cells is 26.74 μM (Fig. 1(C)). It is noteworthy that there exists a substantial disparity in the CC_{50} of TET between PAMs, BMDMs and MA104 cells. This divergence can likely be attributed to the heightened fragility of PAMs and BMDMs, being primary cells, as opposed to the more mature and stable MA104 cells. PAMs and BMDMs are more sensitive to external stimuli, while MA104 cells demonstrate greater survivability to the toxicity of TET at higher concentrations. To mitigate the cytotoxic impact on both PAMs, BMDMs and MA104 cells, the maximum concentration of TET in subsequent trials was 2 μM.

3.2. Anti-ASFV effect of TET in vitro

The experiments were conducted to further identify the inhibitory effect of TET against ASFV. The cells were pretreated with TET for 2 h and then infected with ASFV. The IFA showed that TET significantly reduced the number of ASFV-infected cells in PAMs. At a concentration of 2 μM, hardly any fluorescent PAMs were observed (Fig. 2(A)). Subsequent Western Blot assays demonstrated that TET significantly decreased the expression level of ASFV p72 in cells, showing a dose-dependent inhibition (Fig. 2(B)–(D)). The inhibition rates of TET against ASFV were calculated using Cell-ELISA, and the IC_{50} were determined by non-linear fitting. The IC_{50} of TET against ASFV on PAMs, BMDMs, and MA104 cells were 0.45 μM, 1.15 μM, and 0.87 μM, respectively (Fig. 2(E)).

To rule out the possibility that the dose of virus infection had an effect, we performed assays with ASFV at an MOI of 0.5, 1, 2, or 5 in PAMs as described above. Compared to the level of ASFV-p72 protein in the control cells, the level of ASFV-p72 protein in TET-treated PAMs was significantly reduced at all tested virus title (Fig. 2(F)–(I)), indicating that TET exhibits potent antiviral activity even in the presence of high-title ASFV infection.

3.3. The therapy stage of TET in ASFV infection

The therapy stage of TET on the viral infection of ASFV were further analyzed. According to the aforementioned TOA assay (Fig. 3(A)), TET was tested at a concentration of 2 μM. Both two-stage and three-stage TET treatments significantly inhibited the transcription and protein expression levels of ASFV. The qRT-PCR results showed that TET treatment at each stage of attachment, internalization, and replication (Lane 6–8) could suppress ASFV (Fig. 3(B)), while the Western Blot results indicated that a significant reduction in ASFV p72 expression level was observed only during the internalization stage (Lane 7) (Fig. 3(C)). Taking both sets of results into account, TET is likely to primarily inhibit the internalization stage of ASFV infection.

3.4. The virucidal effect of TET

TET and ASFV were co-incubated at 37 °C for 1 h, with TET concentrations of 0 μM, 2 μM and 4 μM, respectively. Subsequently, TET-pretreated-ASFV was used to infect PAMs, with ASFV infecting TET-pretreated PAMs serving as the control. After 24 h post-infection, RNA was extracted for qRT-PCR analysis. The results demonstrated that the co-incubation of TET and ASFV did not significantly reduce ASFV infection (Fig. 3(D)). The observed weak inhibitory effect of TET against ASFV might be attributed to the partial inhibitory activity displayed by TET present in the ASFV viral suspension during the infection, indicating that TET does not have a direct virucidal effect on ASFV.

3.5. CD1d is not the target of TET

It has been reported that host factor CD1d mediates the entry of ASFV into host cells (Chen et al., 2023). To confirm whether CD1d serves as the target for TET-mediated anti-ASFV activity, knockdown of CD1d

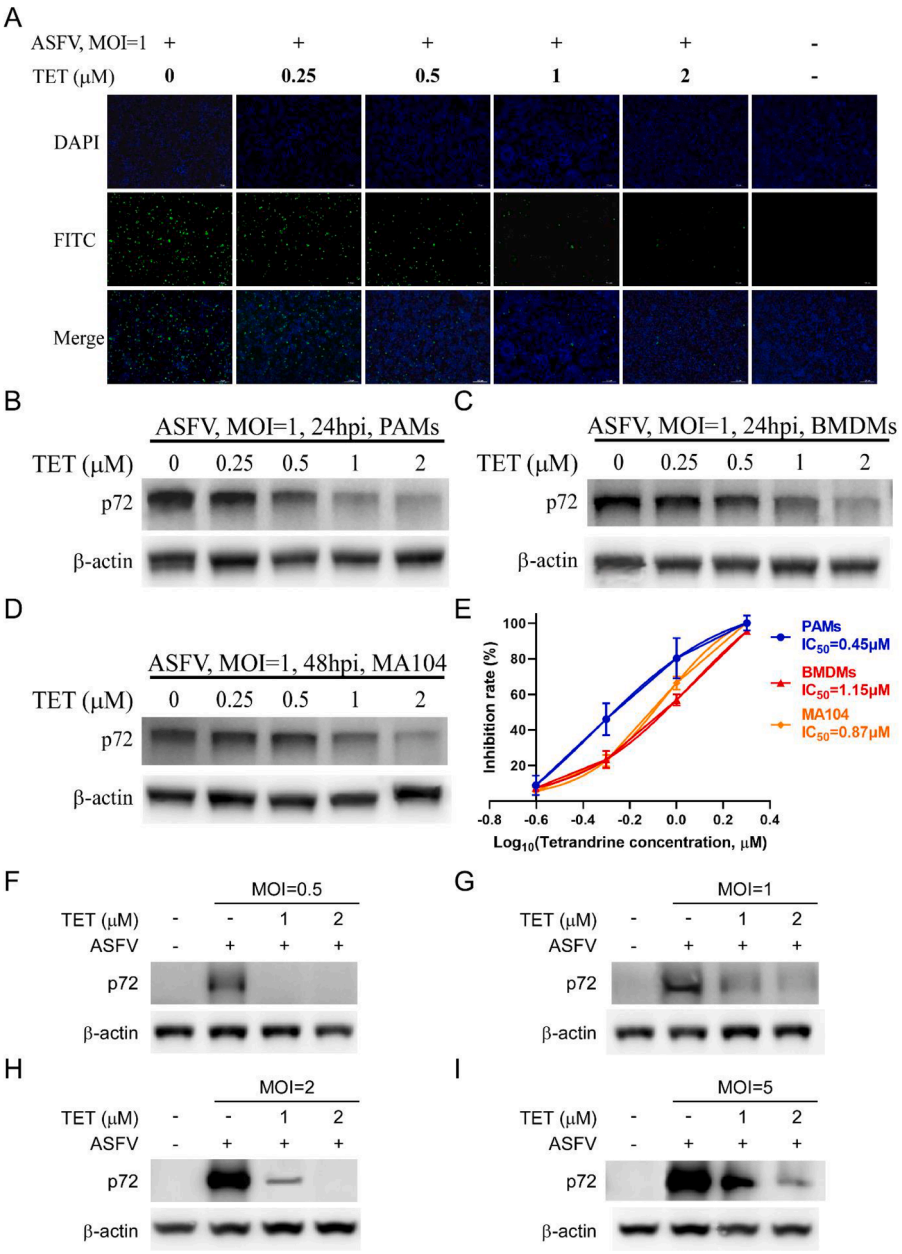

Fig. 2. The anti-ASFV effect and IC_{50} of TET. (A) The anti-ASFV effect of TET on PAMs was analyzed by IFA. Bar = 100 μm. (B-D) The anti-ASFV effect of TET on PAMs, BMDMs and MA104 cells was analyzed by Western Blot. (E) IC_{50} of TET in PAMs, BMDMs and MA104 cells was calculated. Inhibition rate was calculated by Cell-ELISA assay. (F-I) TET reduced infection of different MOI ASFV. TET-preincubated PAMs were incubated with ASFV at an MOI of 0.5, 1, 2, or 5. The expression levels of ASFV-p72 were analyzed by Western Blot.

expression in PAMs was performed by transfecting with specific siRNAs (Fig. 3(E)). Our research findings indicate that in PAMs with reduced CD1d expression, there is a significant decrease in the transcription levels of ASFV viral genome mRNA (Fig. 3(F)). In PAMs with lowered CD1d expression, the ASFV infection level is approximately 10 %, whereas in the TET-treated group, the ASFV infection level is less than 0.5 %, and there is a significant difference between the two groups (***$P < 0.001$). These results suggest that CD1d is not the primary target for the anti-ASFV activity of TET.

3.6. *TET inhibits the macropinocytosis of PAMs*

ASFV can enter cells through clathrin-mediated endocytosis (Hernaez and Alonso, 2010) and macropinocytosis (Sánchez et al., 2012). To investigate the internalization pathway of ASFV inhibited by TET, cellular internalization assays were performed using the clathrin-mediated endocytosis-specific marker transferrin-Alexa594 (Tessier and Woodgett, 2006) and the macropinocytosis-specific marker dextran-Alexa647 (Hua et al., 2006). The endocytosis experiment consisted of two groups: the TET untreated group and the TET treated group. Furthermore, specific inhibitors of clathrin-mediated endocytosis, Chlorpromazine (CPZ), and macropinocytosis-specific inhibitor, Amiloride (AMI), were applied to treat PAMs, serving as positive controls. The results of endocytosis experiment showed no significant difference in transferrin-Alexa594 between the TET-treated group and the untreated group (Fig. 4(A)). However, the Dext fluorescence signal in the TET-treated group completely disappeared compared to the untreated group (Fig. 4(B)), indicating that TET significantly inhibits macropinocytosis.

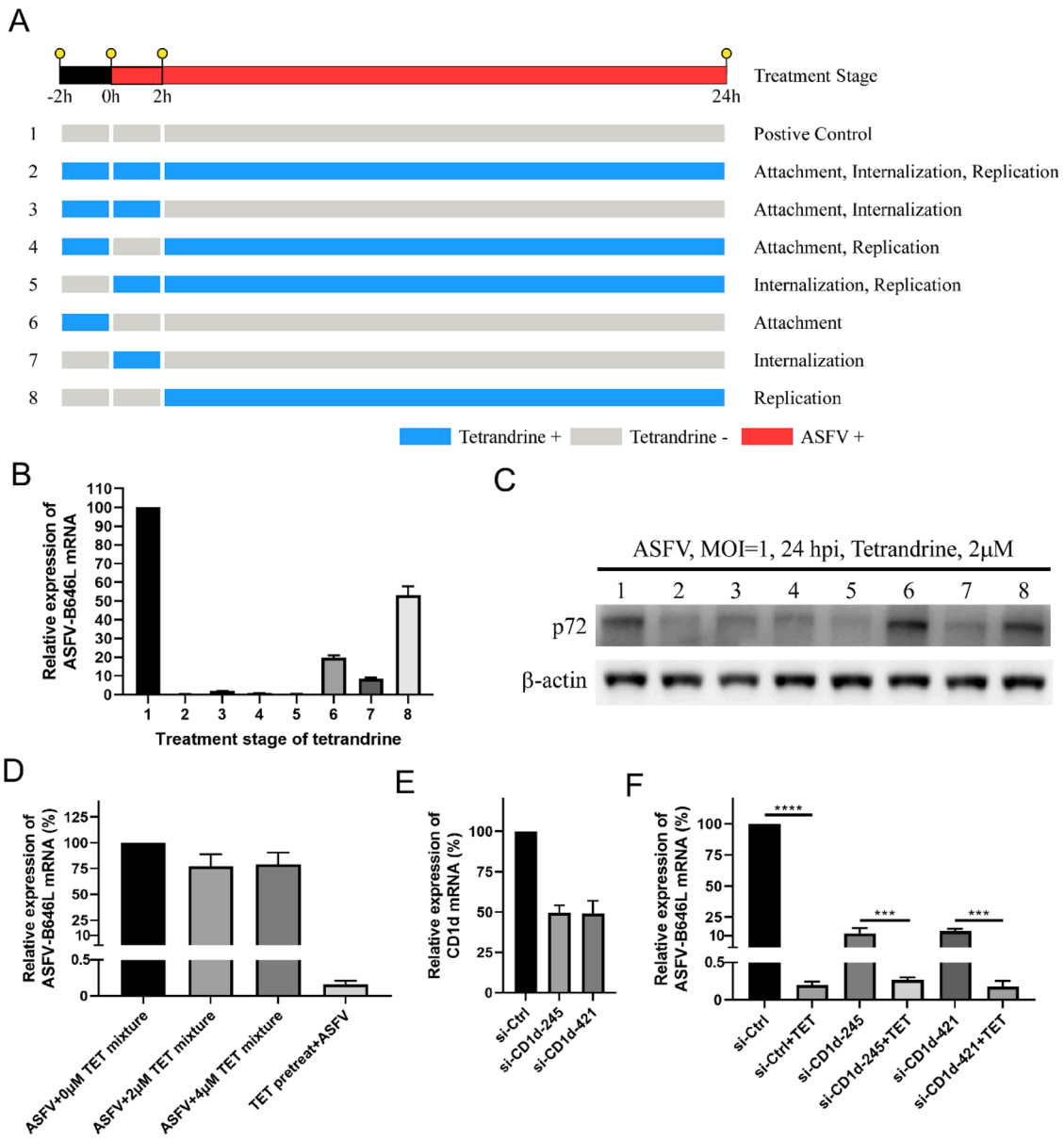

Fig. 3. The therapy stage of TET against ASFV infection on PAMs. (A) The TOA assay was divided into pre-treatment, co-treatment and after-treatment stages. And pre-treatment stage means before ASFV was added, co-treatment stage and after-treatment stage meant after ASFV was added. (B) The experiments were performed following Fig. 3A, and qRT-PCR assay was performed. (C) The experiments were performed following Fig. 3A, and Western Blot assay was performed. (D) qRT-PCR analysis of the TET-pretreated-ASFV infection on PAMs. (E) The mRNA level of CD1d was examined by qRT-PCR. (F) qRT-PCR assay was used to determine whether CD1d was the target of TET. $^{****}P < 0.0001$, $^{***}P < 0.001$.

3.7. ASFV activates PI3K/Akt pathway during internalization

Macropinocytosis of cells is primarily regulated by the PI3K/Akt pathway (Sánchez et al., 2012). In this study, we analyzed the impact of ASFV entry on the PI3K/Akt pathway during the early stages of infection by Western Blot. In PAMs, there was a significant activation of phosphorylated Akt at 5 min, 10 min, and 20 min post-infection with ASFV (Fig. 5(A)). The results in MA104 cells indicate a significant increase in the level of Akt phosphorylation at four time points post-infection (10 min, 20 min, 30 min and 1 h), compared to other time points (Fig. 5(B)). The findings suggest that the early stages of ASFV infection, including attachment and internalization, are associated with the activation of the PI3K/Akt pathway. Furthermore, our ASFV attachment assay revealed no significant differences in Akt phosphorylation level at different time points (Fig. 5(C)), indicating that the internalization of ASFV activates PI3K/Akt pathway.

3.8. TET inhibits the PI3K/Akt pathway

The PAMs were treated with 0 μM TET, 2 μM TET, 1 MOI ASFV, or 1 MOI ASFV + 2 μM TET. After treatment, cell samples were collected at 5 min, 10 min, and 20 min for Western Blot analysis. The results indicated that TET treatment inhibited the phosphorylation of Akt activated during the 20-min internalization of ASFV (Fig. 5(D)).

3.9. LY294002 inhibits macropinocytosis of PAMs

The endocytosis assay included four groups: Ctrl, LY294002, TET, and LY294002 + TET, each group is further divided into ASFV infection group and Mock group. The treatment groups with specific inhibitors of PI3K/Akt, LY294002, as well as the TET and LY294002 + TET combinations, all showed no uptake of dextran-Alexa647 by PAMs (Fig. 6). This suggests that TET and LY294002 effectively inhibit the

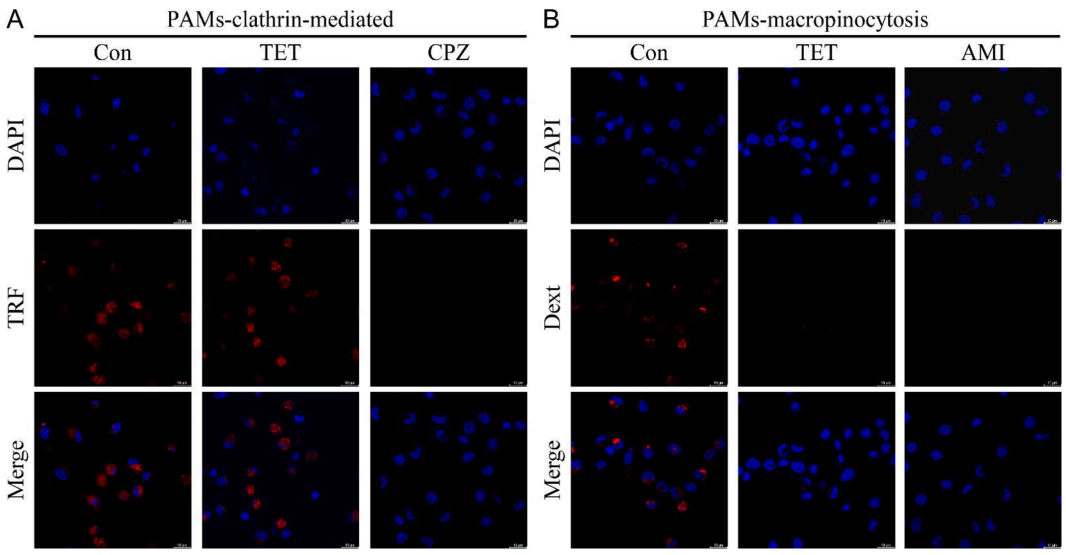

Fig. 4. Endocytosis of PAMs. (A) Clathrin-mediated endocytosis of PAMs. The difference in transferrin-Alexa594 between the TET treatment group and the untreated group showed no statistical significance, indicating that TET does not inhibit the clathrin-mediated endocytosis of PAMs. (B) Macropinocytosis of PAMs. The group treated with TET showed no fluorescence of dextran-Alexa647 compared to the untreated group, indicating that TET inhibited the macropinocytosis of PAMs.

macropinocytosis of PAMs, whether infected with ASFV or not, and these two drugs exhibit similar activity.

3.10. Inhibition of ASFV by TET depends on the PI3K/Akt pathway

To investigate whether the inhibitory effect of TET on ASFV depends on the PI3K/Akt pathway, qRT-PCR, HAD and Western Blot assays were conducted. The results revealed that both LY294002 and TET significantly suppressed the levels of *CP204L* and *B646L* (Fig. 7(A)). Western Blot assays demonstrated that LY294002 and/or TET significantly reduced the levels of ASFV p72. TET partially inhibited the phosphorylation of Akt, while LY294002 completely inhibited Akt phosphorylation. Furthermore, the expression of ASFV p72 was not detected in LY294002 and/or TET-treated groups, and the inhibition rate of ASFV was comparable between the LY294002 and TET treatment groups (Fig. 7(B)). HAD assay showed that the LY294002-treated group was $1 \times 10^{2.33}$ HAD_{50}/mL, the TET-treated group was $1 \times 10^{2.125}$ HAD_{50}/mL, the TET+LY294002-treated group was $1 \times 10^{2.25}$ HAD_{50}/mL, and the untreated group was $1 \times 10^{6.29}$ HAD_{50}/mL (Fig. 7(C)). This indicates a significant reduction in the number of red blood cells adhered to PAMs treated with LY294002 and/or TET. These findings indicate that LY294002 and TET effectively inhibit ASFV infection, and this inhibitory effect is dependent on the PI3K/Akt pathway.

3.11. Illustration of TET exerting its anti-ASFV effect

The schematic diagram illustrates the inhibition of Akt phosphorylation by TET, blocking the entry of ASFV through macropinocytosis. Macropinocytosis is primarily regulated by the PI3K/Akt pathway, where activation of cell membrane surface receptors leads to actin filaments polymerization, forming membrane ruffles that engulf a large amount of extracellular fluid to form macropinosomes (Kay, 2021). TET inhibits the PI3K/Akt pathway, preventing actin polymerization and weakening or abolishing the macropinocytosis. As a result, ASFV cannot utilize this pathway for cell entry, thereby exerting TET's inhibitory effect on ASFV (Fig. 8).

3.12. Broad-spectrum antiviral effects of TET

TET has been demonstrated to possess antiviral activity against the Ebola virus and other virus (Galindo et al., 2021; Sakurai et al., 2015). Further investigations have revealed that TET exhibits no cytotoxicity to Vero, MDBK and IPEC-J2 cells when the concentration is equal to or below 10 μM (Fig. 9(A)). The CC_{50} of TET in Vero cells is 29.03 μM, in MDBK cells is 28.72 μM, and in IPEC-J2 cells is 30.03 μM (Fig. 9(B)). We confirmed the antiviral effects of TET against LSDV and PEDV in Vero, MDBK or IPEC-J2 cells. Western Blot results demonstrated a dose-dependent inhibitory effect of TET on both LSDV and PEDV (Fig. 9 (C)–(F)). The antiviral activity of TET against multiple viruses underscores its potential as a broad-spectrum antiviral drug.

4. Discussion

ASF has spread widely in the world and caused huge economic losses to pig industry. In August 2018, ASF was introduced into China, and rapidly spread to other parts of the country within three months, with more than 50 outbreaks and over 200,000 pigs culled, causing huge economic losses and extremely severe epidemic prevention and control (Ge et al., 2018; Zhou et al., 2018). The lack of available vaccines against ASFV limits the ASFV control to effective management, early diagnosis, and, in the case of wealthy ASF-free areas, the massive culling of infected and in-contact pigs, strategies that are being continuously reviewed (Monteagudo et al., 2017). Therefore, safe and effective drugs against ASFV is crucial in providing timely protection, reducing economic losses, and improving epidemic prevention and control.

Chinese herbal medicines are widely used for the prevention and treatment of viral infectious diseases in China and many other Asian countries. There are a variety of Chinese herbal medicines approved by National Medical Products Administration (NMPA) for the treatment of viral diseases (Li and Peng, 2013). TET is widely utilized component in traditional Chinese medicine and has been shown to have a variety of biological activities, including antibacterial, antiviral, anti-inflammatory and immunomodulatory (Bhagya and Chandrashekar, 2016). The earliest report on the antiviral effect of TET is that it potently inhibits herpes simplex virus type-1-induced keratitis in BALB/c mice (Hu et al., 1997). Liou et al. claimed that TET could attenuate dengue virus in human lung cells (Liou et al., 2008). TET acts as two-pore channels (TPCs) specific blocker could prevent the capsid disassembly and nuclear transport required for virus entry, and strongly inhibits Ebola virus (Sakurai et al., 2015) and Polyomavirus (Dobson et al., 2020). The inhibition of TET against Ebola virus was also verified on the screen of Food and Drug Administration (FDA)-approved drug

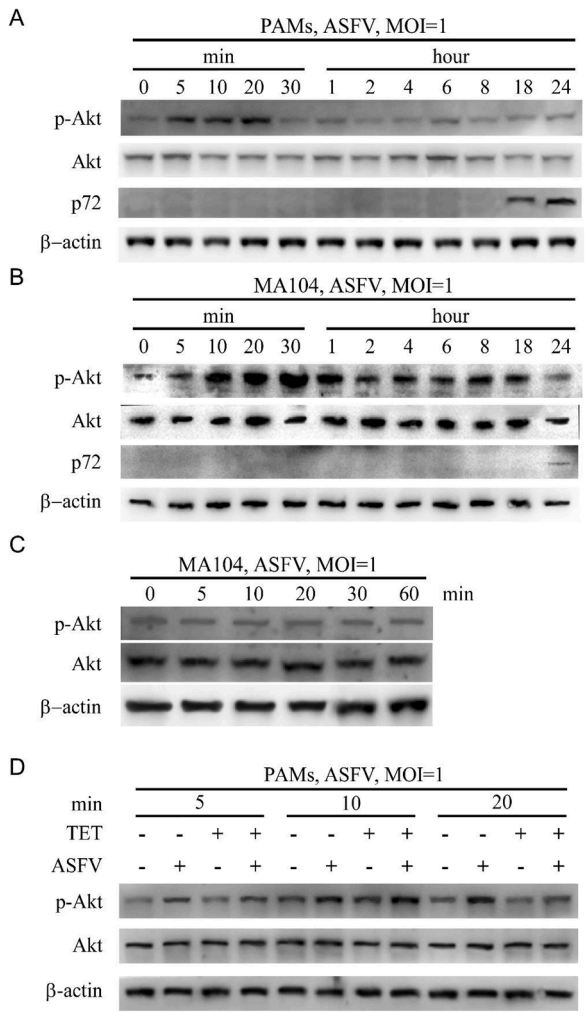

Fig. 5. ASFV induces Akt phosphorylation during internalization. The level of Akt phosphorylation was detected by Western Blot at the indicated time points. (A) The results in PAMs show a significant increase in the level of Akt phosphorylation at three time points post-infection (5 min, 10 min and 20 min), compared to other time points. (B) The results in MA104 cells indicate a significant increase in the level of Akt phosphorylation at four time points post-infection (10 min, 20 min, 30 min and 1 h), compared to other time points. (C) Virus attachment tests were performed on MA104 cells. Western Blot showed that ASFV did not induce Akt phosphorylation during attachment. (D) The phosphorylation level of Akt in the TET treated group was significantly reduced after 20 min, indicating that TET inhibits phosphorylation of Akt and blocks the activation of PI3K/Akt pathway.

library (Du et al., 2020). Mayor et al. screened a drug library using a pseudotype platform encoding enhanced green fluorescent protein (EGFP), and the inhibition of TET with infectious hantaviruses was validated (Mayor et al., 2021). TET also showed antiviral activity against severe acute respiratory syndrome coronavirus 2 (SARS-COV-2) and ASFV in vitro (Galindo et al., 2021; Jeon et al., 2020), indicating its potential to become a broad-spectrum antiviral agent. However, it is essential to note that further studies are still needed to fully understand its mechanisms of action and determine its effectiveness and safety in various clinical applications.

In our study, we demonstrated the antiviral effect of TET on genotype II ASFV China/2018/AnhuiXCGQ in PAMs, BMDMs or MA104 cells. We conducted initial tests with varying concentrations of TET on both PAMs, BMDMs and MA104 cells. The findings revealed that TET exhibited no cytotoxicity to all cells at concentrations of 5 μM or below. To validate the in vitro efficacy of TET against ASFV, we employed IFA and Western Blot. The results indicated that TET exerted a dose-dependent inhibition on ASFV in both cells. The inhibitory rates of various concentrations of TET on ASFV were determined using Cell-ELISA assay and fitting calculations. The IC_{50} of TET against ASFV in PAMs, BMDMs and MA104 cells were determined to be 0.45 μM, 1.15 μM and 0.87 μM, respectively, and TET exhibited a significant inhibitory effect on ASFV at different title.

The TOA assay can be used to analyze the stages of drug therapy. Burghgraeve et al. confirmed that an analogue of the antibiotic teicoplanin prevented flavivirus entry in vitro by TOA assays (De Burghgraeve et al., 2012). Therefore, we utilized the TOA assay to determine the therapy stage of TET in ASFV infection. However, there were discrepancies between the mRNA and protein expression level analyses. Specifically, the $2^{-\Delta\Delta Ct}$ method indicated that TET could reduce ASFV gene transcription at the attachment, internalization, and replication stages. In contrast, Western Blot demonstrated a significant reduction in ASFV infection only at the entry stage following TET treatment. During the virus attachment and replication stages, TET treatment did not lower ASFV protein expression levels. This phenomenon may be attributed to the greater sensitivity of qRT-PCR compared to Western Blot. Therefore, it is hypothesized that TET may primarily inhibit the entry stage of ASFV infection, although it might also exert inhibitory effects on other stages that are not detectable through Western Blot. Considering the combined results of both experiments, it suggests that TET may predominantly inhibit the internalization of ASFV. In addition, given the relatively weak antiviral effect of TET after ASFV entry, TET is not suitable for treating infected animals but is better suited for prevention of the infection. Furthermore, we have ruled out the direct virucidal effect of TET against ASFV. The host factor CD1d facilitates ASFV entry into the host cells via clathrin-mediated endocytosis (Chen et al., 2023). We have also ruled out the possibility of CD1d being the target of TET.

We investigated the specific pathways through which TET inhibits the internalization of ASFV. We performed endocytic test using fluorescently labeled transferrin-Alexa594 and dextran-Alexa647. The results showed that TET had no effect on the internalization of transferrin-Alexa594, but significantly inhibited the internalization of dextran-Alexa647. This suggests that TET can effectively inhibit macropinocytosis, a process by which ASFV enters host cells (Sánchez et al., 2012). These findings offer valuable insights that guide our further investigation into the underlying mechanism of TET's anti-ASFV effect.

ASFV enters host cells through macropinocytosis and activates the PI3K/Akt pathway to promote its own replication. This activation is particularly notable during the internalization, as it greatly enhances the phosphorylation of Akt (Sánchez et al., 2012). The PI3K/Akt pathway is an important cellular signaling pathway that significantly influences cell growth, proliferation, survival, and metabolic regulation (Ersahin et al., 2015). In this study, we confirmed that ASFV infection induces the phosphorylation of Akt in both PAMs and MA104 cells. In PAMs, Akt phosphorylation was activated as early as 5 min in post-ASFV infection, peaked at 20 min, and ceased after 20 min, suggesting that ASFV may entry PAMs within 20 min. In MA104 cells, Akt phosphorylation began at 10 min post-ASFV infection, peaked at 30 min, and continued to activate Akt phosphorylation for up to 1 h. This indicates that PAMs are more susceptible to ASFV compared to MA104 cells. The 1 h of post-ASFV infection includes both attachment and internalization phases, and we confirmed through virus attachment experiments that virus attachment does not induce Akt phosphorylation, thereby confirming the activation of the PI3K/Akt signaling pathway during ASFV internalization.

Furthermore, there are reports indicating that TET exhibits inhibitory effects on multiple signaling pathways, including NF-κB and the PI3K/Akt pathway (Xu et al., 2021). Through the establishment of different TET treatment groups and Western Blot, it was observed that TET can significantly inhibit the activation of the PI3K/Akt pathway at 20 min post-ASFV infection. These findings naturally lead us to contemplate the relationship between the inhibitory effect of TET

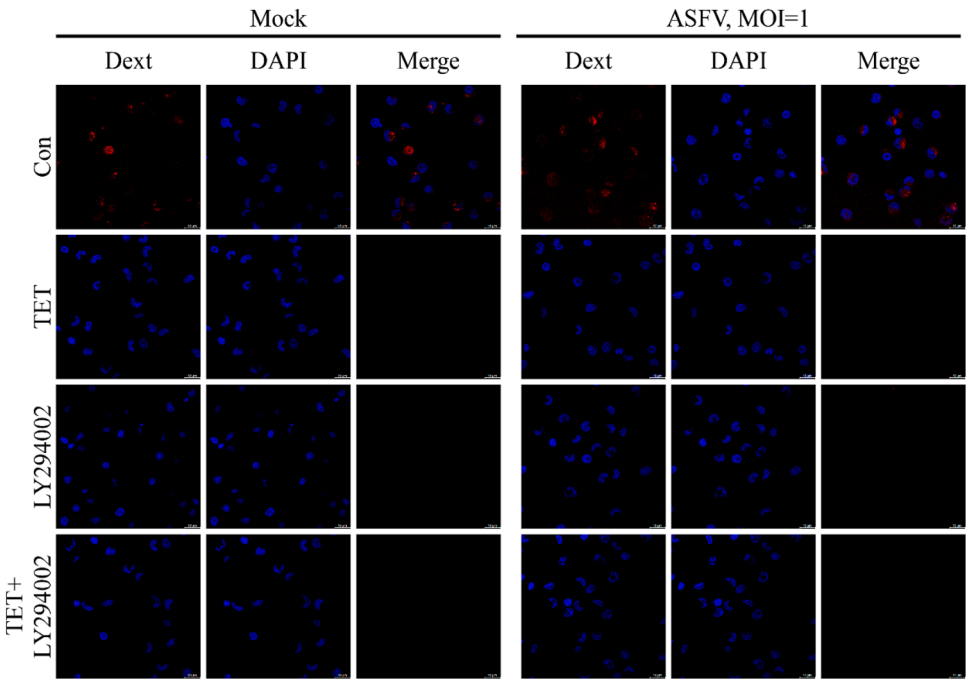

Fig. 6. Dextran-Alexa647 was not observed in groups treated with TET, LY294002 or TET+LY294002, it indicated that TET and LY294002 blocked macropinocytosis of PAMs.

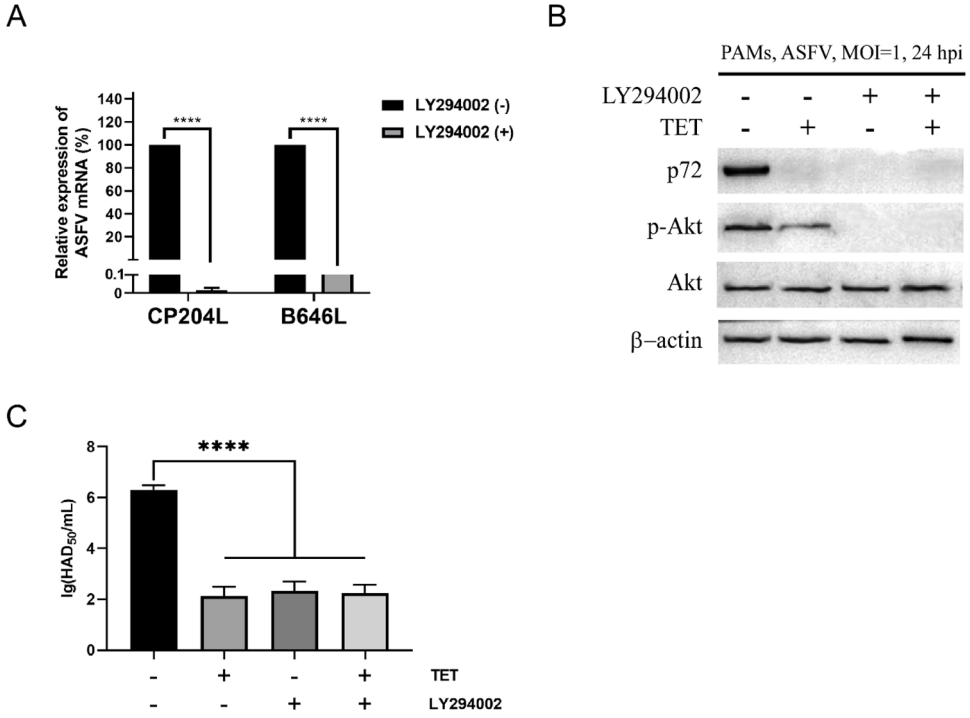

Fig. 7. LY294002 can inhibit ASFV. (A) The expression level of ASFV *CP204L* and *B646*L in PAMs was detected by qRT-PCR assay. (B) Western Blot and (C) HAD assays showed that the expression level of ASFV decreased significantly after TET, LY294002 or TET + LY294002 treatment. Statistical significance is denoted by $^{****}P < 0.0001$.

against ASFV and the PI3K/Akt pathway.

Subsequently, we found that the PI3K/Akt pathway-specific inhibitor LY294002 exhibits a similar inhibitory effect on macropinocytosis as TET. qRT-PCR, HAD, and Western Blot assays revealed a significant reduction of ASFV in the LY294002 treatment group, indicating the effective inhibition of LY294002 on ASFV. Compared to the LY294002 control group, the inhibition rate of TET on ASFV was nearly 0 %. There was no significant difference in the inhibitory effects on ASFV between the LY294002 + TET co-treatment group and the TET treatment group, suggesting that the inhibitory effect of TET against ASFV is dependent on blocking the macropinocytosis of cells by inhibiting the PI3K/Akt pathway. The inhibitory activity of TET on LSDV and PEDV was validated in Vero, BMDMs or IPEC-J2 cells, demonstrating effective inhibition of these two viruses at safe concentrations and highlighting the

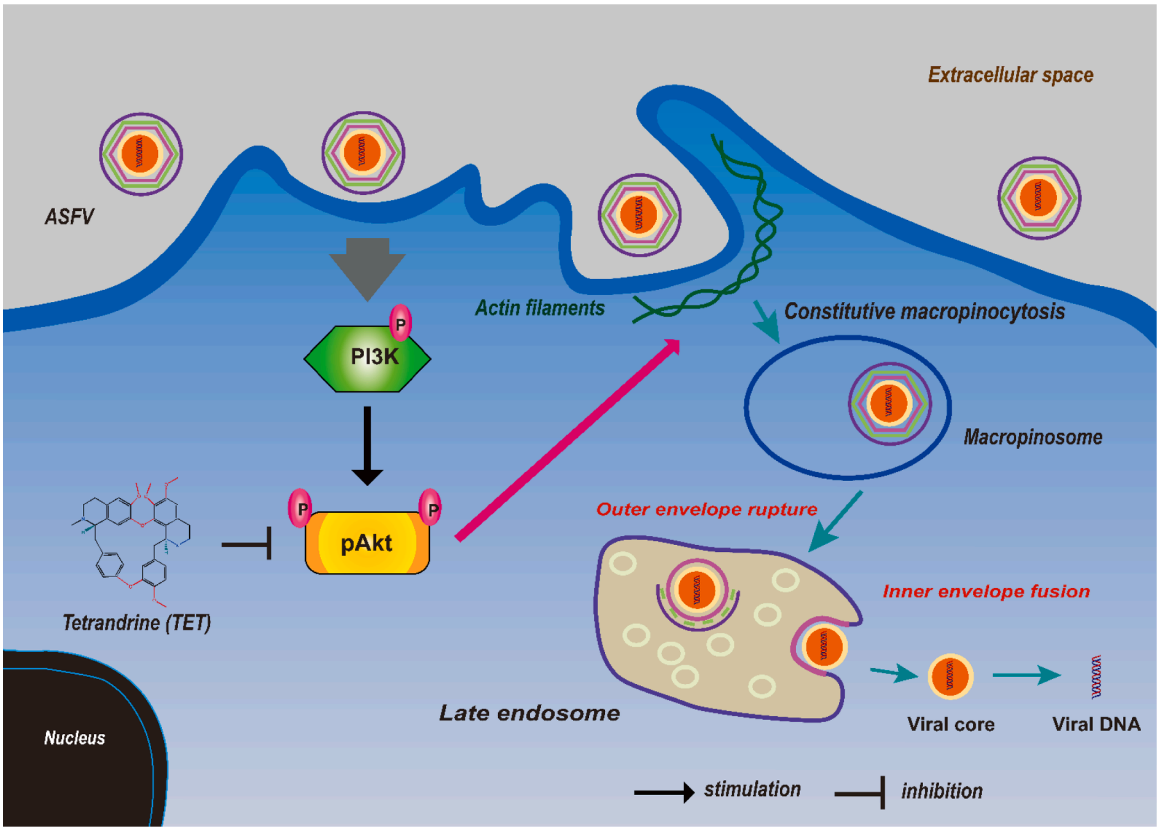

Fig. 8. Schematic diagram of TET inhibiting macropinocytosis of PAMs and ASFV entry.

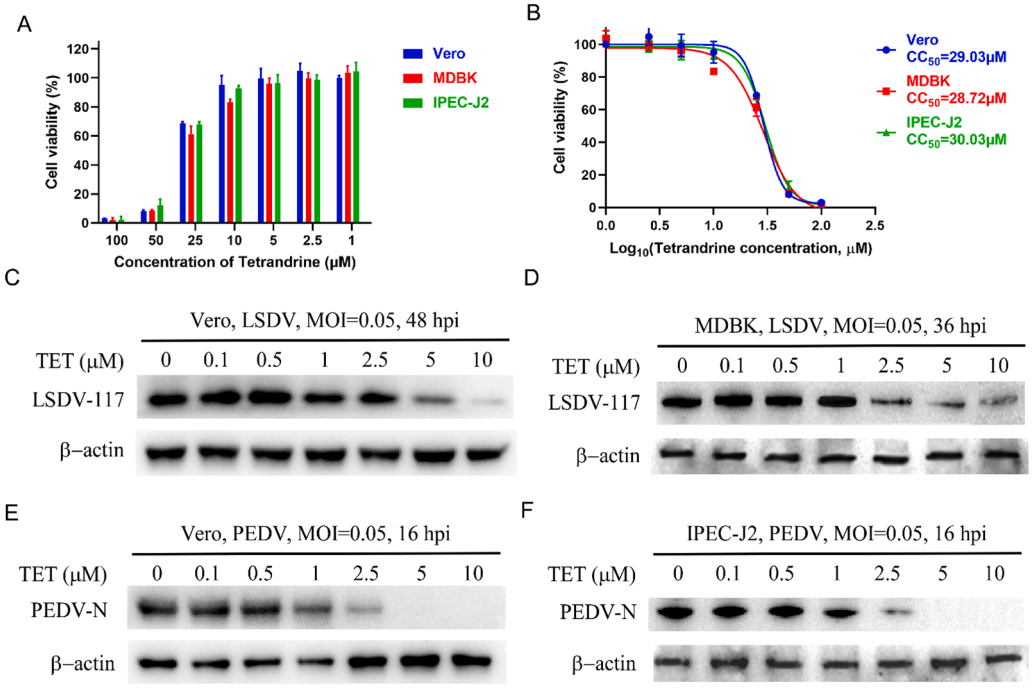

Fig. 9. Broad-spectrum antiviral activity of TET. (A) Cell viability of cells (Vero, MDBK and IPEC-J2) treated with TET at the indicated concentration. (B) CC_{50} of TET on Vero, MDBK and IPEC-J2 cell. Western Blot assay showed that the protein level of (C-D) LSDV 117 and (E-F) PEDV N decreased significantly in a dose-dependent manner after TET treatment.

potential of TET as a broad-spectrum antiviral drug.

In conclusion, TET, as a compound with multiple biological activities, may be a potential therapeutic option against ASFV. This study provided initial insights into the anti-ASFV mechanism of TET, revealing its potential to exert its antiviral effect by inhibiting the PI3K/Akt pathway. This provides strong support for the development and

application of TET in the field of disease treatment, and lays the foundation for further investigation into its antiviral mechanisms as well as preclinical and clinical trials. Future research should focus on developing anti-ASFV drugs targeting the PI3K/Akt pathway and evaluating their feasibility for practical applications. This will contribute to the development of new prevention and control strategies in the pig industry, reducing ASFV transmission and pig population infections, thereby mitigating economic losses and promoting the overall health of the livestock sector.

5. Conclusion

In conclusion, TET possesses significant anti-ASFV properties. ASFV enters the cell through PI3K/Akt pathway and then replicates, and TET can inhibit the entry of ASFV by inhibiting this pathway, thus acting as a virus suppressor. Further research is warranted to fully elucidate the molecular mechanisms underlying TET's anti-ASFV effects and implications for the subsequent research and development of anti-ASFV drugs targeting PI3K/Akt pathway. Additionally, exploring TET's potential as a broad-spectrum antiviral agent against a range of viruses would be worthwhile.

Author statement

Generative AI and AI-assisted technologies were not used in the writing of this manuscript.

Author contribution statement

Conceptualization was carried out by XF and QBX. Funding acquisition and project administration were managed by XF, WXD, DJJ and WZL. Validation, visualization, writing-original draft and writing-review & editing were performed by QBX, LC and MYR. Data curation was performed by HXJ, ZDX, ZDX, GMX, ZYL, LK and HYX. All authors contributed to the article and approved the submitted version.

Funding statement

This research was funded by the National Project for the Prevention and Control of major exotic animal diseases (2022YFD1800500), the National Key Research and Development Program of China (2021YFD1800500), Hainan Province Science and Technology Special Fund (ZDYF2022XDNY248), the Jiangsu Agricultural Science and Technology Independent Innovation Fund Project [CX (21) 2038], the Sanya Nanjing Agricultural University Research Institute Guiding Fund Project (NAUSY-ZD08).

Declaration of Competing Interest

The authors declare that they have no known competing financial interests or personal relationships that could have appeared to influence the work reported in this paper.

Data availability

Data will be made available on request.

Acknowledgments

We thank the China Animal Health and Epidemiology Center for providing the biomaterial and BSL-3 laboratory. Many thanks to Director Jinming Li for his kind and warm help.

References

Bhagya, N., Chandrashekar, K.R., 2016. Tetrandrine—A molecule of wide bioactivity. Phytochemistry 125, 5–13.
Cackett, G., Matelska, D., Sýkora, M., Portugal, R., Malecki, M., Bähler, J., Dixon, L., Werner, F., 2020. The African swine fever virus transcriptome. J. Virol. 94, e00119–e00120.
Chen, K.K., Chen, A.L., 1935. The alkaloids of Han-Fang-Chi. J. Biol. Chem. 109, 681–685.
Chen, X., Zheng, J., Liu, C., Li, T., Wang, X., Li, X., Bao, M., Li, J., Huang, L., Zhang, Z., Bu, Z., Weng, C., 2023. CD1d facilitates African swine fever virus entry into the host cells via clathrin-mediated endocytosis. Emerg Microbes Infect. 12, 2220575.
De Burghgraeve, T., Kaptein, S.J., Ayala-Nunez, N.V., Mondotte, J.A., Pastorino, B., Printsevskaya, S.S., de Lamballerie, X., Jacobs, M., Preobrazhenskaya, M., Gamarnik, A.V., Smit, J.M., Neyts, J., 2012. An analogue of the antibiotic teicoplanin prevents flavivirus entry in vitro. PLoS One 7, e37244.
Dixon, L.K., Sun, H., Roberts, H., 2019. African swine fever. Antivir. Res. 165, 34–41.
Dobson, S.J., Mankouri, J., Whitehouse, A., 2020. Identification of potassium and calcium channel inhibitors as modulators of polyomavirus endosomal trafficking. Antivir. Res. 179, 104819.
Du, X., Zuo, X., Meng, F., Wu, F., Zhao, X., Li, C., Cheng, G., Qin, F.X., 2020. Combinatorial screening of a panel of FDA-approved drugs identifies several candidates with anti-Ebola activities. Biochem. Biophys. Res. Commun. 522, 862–868.
Ersahin, T., Tuncbag, N., Cetin-Atalay, R., 2015. The PI3K/AKT/mTOR interactive pathway. Mol. Biosyst. 11, 1946–1954.
Eustace Montgomery, R., 1921. On a form of swine fever occurring in British East Africa (Kenya Colony). J. Comp. Pathol. Ther. 34, 159–191.
Galindo, I., Garaigorta, U., Lasala, F., Cuesta-Geijo, M.A., Bueno, P., Gil, C., Delgado, R., Gastaminza, P., Alonso, C., 2021. Antiviral drugs targeting endosomal membrane proteins inhibit distant animal and human pathogenic viruses. Antivir. Res. 186, 104990.
Gallardo, M.C., Reoyo, A.T., Fernández-Pinero, J., Iglesias, I., Muñoz, M.J., Arias, M.L., 2015. African swine fever: a global view of the current challenge. Porcine Health Manag. 1, 21.
Ge, S., Li, J., Fan, X., Liu, F., Li, L., Wang, Q., Ren, W., Bao, J., Liu, C., Wang, H., Liu, Y., Zhang, Y., Xu, T., Wu, X., Wang, Z., 2018. Molecular characterization of African swine fever virus, China, 2018. Emerg. Infect. Dis. 24, 2131–2133.
Hernaez, B., Alonso, C., 2010. Dynamin- and clathrin-dependent endocytosis in African swine fever virus entry. J. Virol. 84, 2100–2109.
Hu, S., Dutt, J., Zhao, T., Foster, C.S., 1997. Tetrandrine potently inhibits herpes simplex virus type-1-induced keratitis in BALB/c mice. Ocul. Immunol. Inflamm. 5, 173–180.
Hua, W., Sheff, D., Toomre, D., Mellman, I., 2006. Vectorial insertion of apical and basolateral membrane proteins in polarized epithelial cells revealed by quantitative 3D live cell imaging. J. Cell Biol. 172, 1035–1044.
Jeon, S., Ko, M., Lee, J., Choi, I., Byun, S.Y., Park, S., Shum, D., Kim, S., 2020. Identification of antiviral drug candidates against SARS-CoV-2 from FDA-approved drugs. Antimicrob. Agents Chemother. 64, e00819–e00820.
Kay, R.R., 2021. Macropinocytosis: biology and mechanisms. Cells Dev. 168, 203713.
Knudsen, R.C., Genovesi, E.V., Whyard, T.C., Wool, S.H., 1987. Cytopathogenic effect of African swine fever virus for pig monocytes: characterization and use in microassay. Vet. Microbiol. 14, 15–24.
Li, T., Peng, T., 2013. Traditional Chinese herbal medicine as a source of molecules with antiviral activity. Antivir. Res. 97, 1–9.
Liou, J.T., Chen, Z.Y., Ho, L.J., Yang, S.P., Chang, D.M., Liang, C.C., Lai, J.H., 2008. Differential effects of triptolide and tetrandrine on activation of COX-2, NF-kappaB, and AP-1 and virus production in dengue virus-infected human lung cells. Eur. J. Pharmacol. 589, 288–298.
Liu, T., Liu, X., Li, W., 2016. Tetrandrine, a Chinese plant-derived alkaloid, is a potential candidate for cancer chemotherapy. Oncotarget 7, 40800–40815.
Mayor, J., Torriani, G., Engler, O., Rothenberger, S., 2021. Identification of novel antiviral compounds targeting entry of hantaviruses. Viruses 13, 685.
Monteagudo, P.L., Lacasta, A., López, E., Bosch, L., Collado, J., Pina-Pedrero, S., Correa-Fiz, F., Accensi, F., Navas, M.J., Vidal, E., Bustos, M.J., Rodríguez, J.M., Gallei, A., Nikolin, V., Salas, M.L., Rodríguez, F., 2017. BA71ΔCD2: a new recombinant live attenuated african swine fever virus with cross-protective capabilities. J. Virol. 91, e01058–17.
Sakurai, Y., Kolokoltsov, A.A., Chen, C.C., Tidwell, M.W., Bauta, W.E., Klugbauer, N., Grimm, C., Wahl-Schott, C., Biel, M., Davey, R.A., 2015. Ebola virus. Two-pore channels control Ebola virus host cell entry and are drug targets for disease treatment. Science 347, 995–998.
Sánchez, E.G., Quintas, A., Pérez-Núñez, D., Nogal, M., Barroso, S., Carrascosa Á, L., Revilla, Y., 2012. African swine fever virus uses macropinocytosis to enter host cells. PLoS Pathog. 8, e1002754.
Tessier, M., Woodgett, J.R., 2006. Role of the Phox homology domain and phosphorylation in activation of serum and glucocorticoid-regulated kinase-3. J. Biol. Chem. 281, 23978–23989.
Van Loock, M., Van den Eynde, C., Hansen, J., Geluykens, P., Ivens, T., Sauviller, S., Bunkens, L., Van Acker, K., Nijs, E., Dams, G., 2013. An automated time-of-drug-addition assay to routinely determine the mode of action of HIV-1 inhibitors. Assay Drug Dev. Technol. 11, 489–500.
Wang, N., Yang, S., Tan, T., Huang, Y., Chen, Y., Dong, C., Chen, J., Luo, X., 2021. Tetrandrine suppresses the growth of human osteosarcoma cells by regulating multiple signaling pathways. Bioengineered 12, 5870–5882.

Xian, Y., Xiao, C., 2020. The structure of ASFV advances the fight against the disease. Trends Biochem. Sci. 45, 276–278.
Xu, W., Chen, S., Wang, X., Tanaka, S., Onda, K., Sugiyama, K., Yamada, H., Hirano, T., 2021. Molecular mechanisms and therapeutic implications of tetrandrine and cepharanthine in T cell acute lymphoblastic leukemia and autoimmune diseases. Pharmacol. Ther. 217, 107659.
Zhou, X., Li, N., Luo, Y., Liu, Y., Miao, F., Chen, T., Zhang, S., Cao, P., Li, X., Tian, K., Qiu, H.J., Hu, R., 2018. Emergence of African swine fever in China, 2018. Transbound. Emerg. Dis. 65, 1482–1484.